ISSN 1560-8034, 1605-6582 (On-line), SPQEO, 2019. V. 22, N 3. P. 338-342.

Mueller polarimetry of discontinuous gold films

O.V. Makarenko[1], A.L. Yampolskiy[1], V.V. Lendiel[1], L.V. Poperenko[1], V.O. Lysiuk[2]

[1]*Taras Shevchenko Kyiv National University, Department of Physics,*
4, Hlushkova ave., 03022 Kyiv, Ukraine
[2]*V. Lashkaryov Institute of Semiconductor Physics, National Academy of Sciences of Ukraine,*
45, prospect Nauky, 03680 Kyiv, Ukraine
E-mail: uv365nm@ukr.net

Abstract. The problem of controlling morphology of discontinuous gold films by the method of optical angular Mueller-polarimetry has been considered. A set of the samples of such films with different amounts of sputtered metal has been fabricated and studied. The reference structure control was carried out by atomic force microscopy and measurement of the film resistivity. In this paper, only 4 elements of the upper left minor of the Mueller matrix have been discussed. It has shown that clear correlation between these elements and the amount of sputtered metal takes place. The two diagonal elements increase with the growth of the metal layer, while the other two demonstrate non-monotonic behavior. The dependences on the angle of light incidence for the diagonal elements are monotonic, and for the non-diagonal ones are opposite. The obtained results may be explained by the features of light scattering in the vicinity of the percolation threshold of an island gold film.

Keywords: polarimetry, Mueller matrix, atomic force microscopy, sensor.

https://doi.org/10.15407/spqeo22.03.338
PACS 78.20.-e, 78.66.-w, 78.68.+m, 81.70.-q

Manuscript received 12.07.19; revised version received 06.08.19; accepted for publication 04.09.19; published online 16.09.19.

1. Introduction

Thin films of gold are an important component of modern technology, and their role continues to grow. Widespread use of gold has taken place in plasmonics, where, due to its high optical conductivity and stability to the action of external factors, it is used as a material for creation of various bio- and chemical sensors [1, 2], plasmon nanoantennas [3, 4], medical and nutritional applications [5], *etc*. It is extremely important in this case to achieve the reproducible metal structure [6], the difficulties in this direction are one of the main factors inhibiting the propagation of biosensor devices. In addition, some types of sensors require a specific structure of the material, for example, nano-spatial [7] or porous [8, 9] gold. Therefore, it is natural that existing methods of morphological control of metallic nanostructures require continuous improvement and addition.

Direct methods for controlling the surface structure are atomic force and scanning electron microscopy. Their disadvantages are contact (for the first) and inadequacy to provide serial control of products. In addition, they do not provide information about the optical properties of the controlled object. Optical polarization techniques such as ellipsometry are more flexible. They are contactless, non-destructive, expressive and can be integrated into other experimental or technological equipment. However, the extremely high sensitivity of the ellipsometry to the state of surfaces imposes specific requirements for the purity of the experiment, as well as a thorough choice of the theoretical model.

In conventional ellipsometry, it is assumed that the registered radiation is completely polarized. However, for a number of objects, one of which is the island metal films, scattering of the probe beam also occurs [10], as a result of which its depolarization can be significant. These cases require an expanded method for measuring the state of polarization using the more powerful Stokes vector formalism [11]. The investigated object is then characterized by a real 4×4 Mueller matrix.

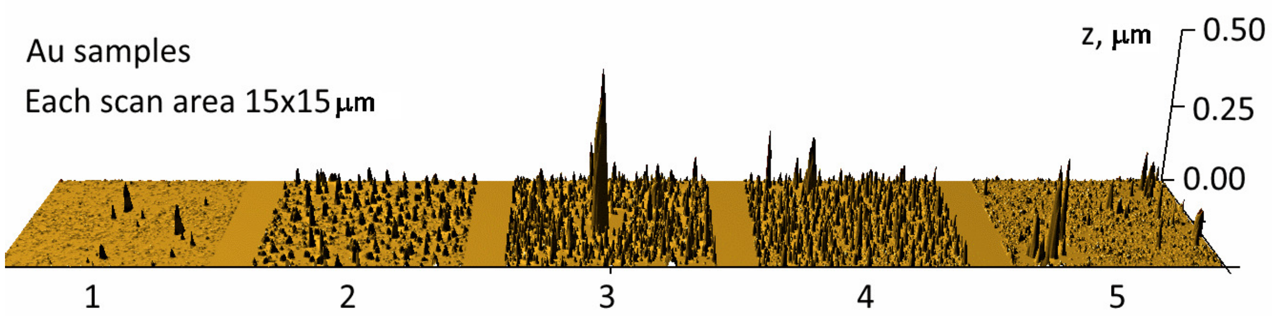

Fig. 1. AFM-images of a set of 5 samples of island gold films.

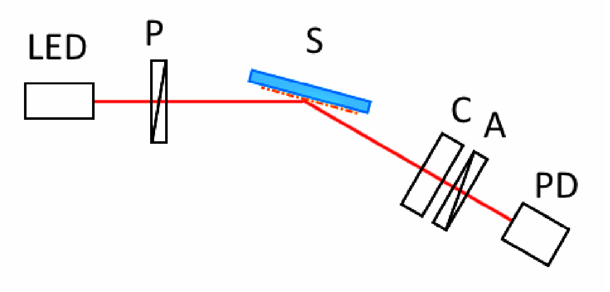

Fig. 2. Optical circuit for polarimetric measurements. LED – source of radiation, P – polarizer, S – sample, C – compensator (quarter-wave phase plate), A – analyzer, PD – photodetector.

The purpose of this work was to study the relation between the individual elements of the Mueller matrix and the structure of island gold films.

2. Experimental

A set of five island gold films with different thicknesses have been prepared. As a substrate, microscopic objective glasses were applied. Formation of samples was carried out in the modernized installation of vacuum spray VUP-5 by magnetron sputtering. The pressure in the chamber at this time was 5×10^{-1} mm Hg, operating current – 20 mA. The thickness of the metal in the process of spraying was not controlled. In total, 5 samples were made.

Morphology of the formed films was controlled using atomic force microscopy and the INTEGRA complex produced by NT-MDT. The 15×15 μm areas with a resolution of 40 nm on the surface of each sample were scanned. Their appearance is presented in Fig. 1.

As it can be seen from this figure, the metal layer grows, while the height and number of irregularities on its surface pass through the extremum. The highest roughness is observed for the samples 3 and 4, while the samples 1 and 5 have a smoother surface. The task of this work was to investigate the optical properties of these surfaces. For additional control of the integrity of this island structure, measurements of the resistivity of the fabricated metal films were performed using the four-probe method. Note that, for the samples 1 and 2, any noticeable conductivity was not detected, so it is likely that these films did not reach the percolation threshold. Also, the thickness of the metal layer was approximated by measuring the optical transmittance at the wavelength $\lambda = 625$ nm. For simplicity, only a single reflection from a glass substrate was taken into account. Since we obtain an effective thickness value, the optical parameters of gold were taken for a bulk metal ($n = 0.175$, $k = 3.392$ [12]). Table shows the number of irregularities above the threshold of about 25% of the maximum height recorded on the surface of each sample, and their average size, film resistance, transmission, and estimated thickness d_{eff}.

Table. Controlled sample parameters

	AFM		Electrical parameter	Transmittance	
Sample	Number of irregularities	Their average size, nm	Resistivity, 10^{-6} Ohm·m	T	Thickness d_{eff}, nm
1	15	215	–	0.76	3.1
2	228	194	–	0.62	6.1
3	613	146	20	0.48	9.7
4	701	158	30	0.52	8.6
5	64	173	8.2	0.26	18

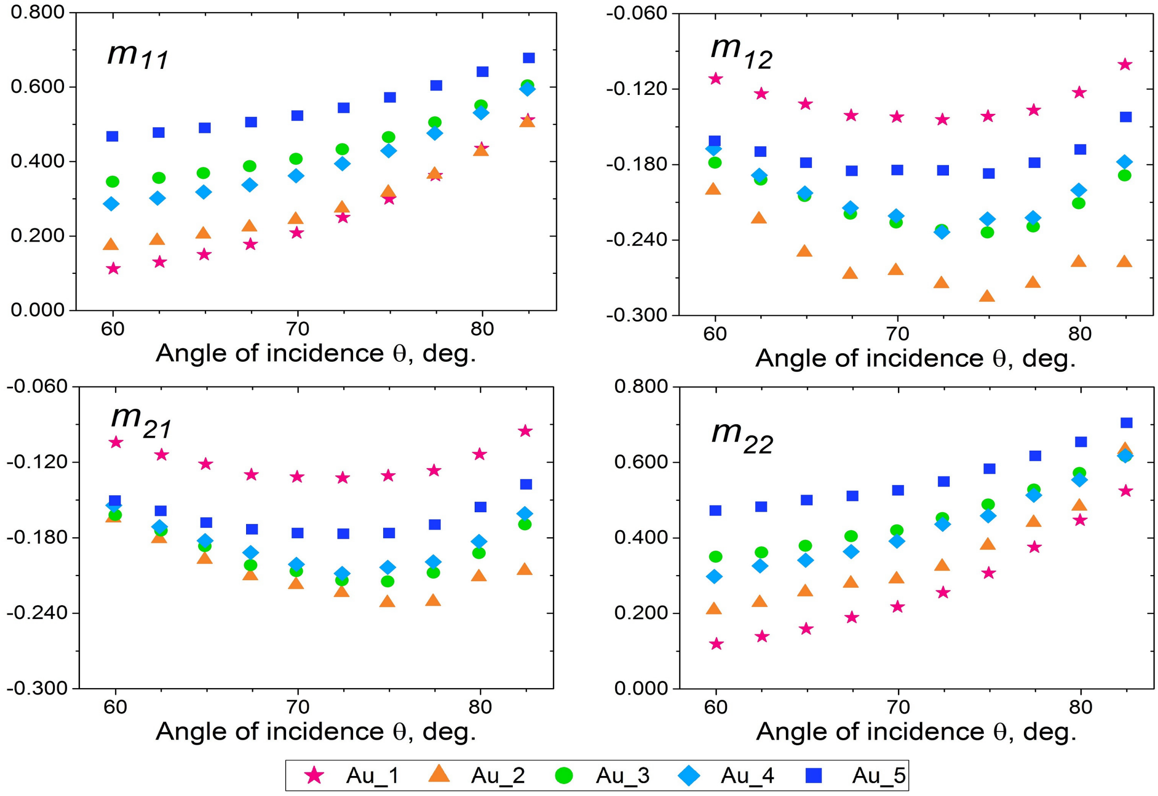

Fig. 3. Angular dependences for elements of upper left minor of the Mueller matrix of studied samples of island films.

Optical polarimetry was performed on an automated goniopolarimetric complex [13]. Its configuration during the research was as shown in Fig. 2.

The operation radiation wavelength was 625 nm. The flat-polarized light drops at a given angle θ on the metal film S. Changing the angular positions of the phase plate C and analyzer A and recording the corresponding beam intensities on the PD receiver, the four components of the reflected beam Stokes vector were measured $\vec{S}=\{I,Q,U,V\}^T$. Additional turns of the polarizer P and measurement of the Stokes vector in the absence of the sample made it possible to determine the Mueller matrix of the sample at this angular position.

A well-known approach [14] is used for this, when the matrix equation that relates the Stokes vectors of the incident $(\vec{S}_{01})$ and reflected $(\vec{S}_1)$ radiation can be rewritten in the following modified form:

$$\vec{S}_1=\hat{M}\vec{S}_{01}\rightarrow\begin{bmatrix}\vec{S}_{01}^T & & & \\ & \vec{S}_{01}^T & & \\ & & \vec{S}_{01}^T & \\ & & & \vec{S}_{01}^T\end{bmatrix}\cdot\begin{bmatrix}m_{11}\\ m_{12}\\ m_{13}\\ \vdots\\ m_{44}\end{bmatrix}=\vec{S}_1 .$$

The matrix 4×16 on the left side of the modified equation is formed from the elements of the Stokes vector of the incident beam (in empty positions there are zeros), and the vector is from the strings of the desired Mueller matrix $\hat{M}$. We have an incomplete system of 4 linear equations with 16 variables. To solve the system, it is supplemented by new equations with other input vectors: $\vec{S}_{02}^T$, $\vec{S}_{03}^T$, and so on (with other positions of the polarizer). Accordingly, the vector in the right side expands:

$$\begin{bmatrix}\vec{S}_{01}^T & & & \\ & \vec{S}_{01}^T & & \\ & & \vec{S}_{01}^T & \\ & & & \vec{S}_{01}^T\\ \vec{S}_{02}^T & & & \\ & \vec{S}_{02}^T & & \\ & & \vec{S}_{02}^T & \\ & & & \vec{S}_{02}^T\\ & \vdots & & \end{bmatrix}\cdot\begin{bmatrix}m_{11}\\ m_{12}\\ m_{13}\\ \vdots\\ m_{44}\end{bmatrix}=\begin{bmatrix}\vec{S}_1\\ \vec{S}_2\\ \vdots\end{bmatrix}.$$

During the measurements, the analyzer always remained oriented parallel to the plane of incidence

(p-plane). The choice of the elements of the Mueller matrix depends on the chosen positions of the polarizer and the phase plate, which is determined by the condition number of the matrix of the system of linear equations and the accuracy of the components of the Stokes vector [14, 15]. In our experiment, the angular positions of these elements acquired values –45°, 0°, 30°, 60° and 90°. Thus, each Stokes vector was measured using 5 equations, and the system for finding elements of the Mueller matrix contained 20 equations. The redundancy of measurements increases the accuracy of results obtained, but takes more time. In addition, the measurement of the intensity of light at the outlet has a significant effect on the final results. During the experiment, the accumulation of the signal from the photodetector continued until the relative error of 0.1% achievement.

3. Results and discussion

For each gold sample, measurements of the elements of the Mueller matrix were performed using the above-described procedure, which was accompanied by angle scanning. The range of change in angle of incidence of the probe beam was $\theta = 60°...82°$.

In [16], the effect of thermal annealing of a golden film on the Mueller matrix was considered. The most sensitive to the state of the surface were the elements m_{12} and m_{21}, which characterize the dependence of the extinction of the environment on the polarization of the incident radiation. Therefore, in our work for the characterization of gold films, the main attention was focused on the left upper minor of this matrix. Fig. 3 shows the angular dependences of the corresponding elements of the Mueller non-standardized matrix for all 5 samples.

From the following series of graphs, it is clear that there is a clear dependence of these coefficients on the amount of deposited metal. Thus, the first element m_{11} that determines the overall reflection increases with an increase in the thickness of the gold layer, which is quite natural. A similar behavior is observed for the element m_{22}. As the angle of incidence increases, the values of these elements increase.

The elements m_{21} and m_{12} show more complex behavior and have a negative sign. They first decrease and then increase with increasing the thickness of the metal layer. The curves for the sample 2 that is close to the percolation threshold lie at the bottom. Angular dependences of these elements also change non-monotonously. They have a minimum of about 75°, and the higher the curve is, the less it becomes wider, lighter and shifts to the region of smaller angles.

4. Conclusions

Thin island films of gold show a change in the extinction coefficient, which is expressed in the behavior of the elements m_{11} and m_{22} of their Mueller matrix. The angular dependences of the elements m_{12} and m_{21} have a non-monotonic behavior with the minimum located in the range 70°...75°. With the growth of the metal layer thickness, these elements minima move to smaller angles of incidence, and in the whole the curves shift upwards.

Such behavior demonstrates the dependence of these elements on the number of scattering centers on the surface. For the samples with more irregularities, the absolute values of m_{12} and m_{21} exceed the corresponding absolute values of elements for isolated islands (sample 1) and continuous film (sample 5). To the authors mind, this may be explained by changes in the origin of the light scattering when the film grows. During this process, mutual influence of metal islands increases and formation of a single connected structure takes place.

Thus, the elements m_{12} and m_{21} of the Mueller matrix for island gold films can provide some information on their morphology, which is an advantage over simpler thickness-controlling methods, such as transmission photometry. Analysis of other elements of the matrix may be promising to obtain additional information on the shape and orientation of surface irregularities.

References

1. Han X., Liu K., & Sun C. Plasmonics for Biosensing. *Materials*. 2019. **12**, No 9. P. 1411. https://doi.org/10.3390/ma12091411.
2. Prabowo B., Purwidyantri A., & Liu K.-C. Surface plasmon resonance optical sensor: A review on light source technology. *Biosensors*. 2018. **8**, No 3. P. 80. https://doi.org/10.3390/bios8030080.
3. Giannini V., Fernández-Domínguez A.I., Heck S.C., & Maier S.A. Plasmonic nanoantennas: Fundamentals and their use in controlling the radiative properties of nanoemitters. *Chem. Rev.* 2011. **111**, No 6. P. 3888–3912. https://doi.org/10.1021/cr1002672.
4. Feichtner T., Selig O., & Hecht B. Plasmonic nanoantenna design and fabrication based on evolutionary optimization. *Opt. Exp.* 2017. **25**, No 10. P. 10828. https://doi.org/10.1364/oe.25.010828.
5. Mukhtar W.M., Ayob N.R., Halim R.M. *et al*. Effect of noble metal thin film thicknesses on surface plasmon resonance (SPR) signal amplification. *J. Adv. Res. in Mater. Sci*. 2018. **49**, No 1. P. 1–9.
6. McPeak K.M., Jayanti S.V., Kress S.J.P. *et al*. Plasmonic films can easily be better: Rules and recipes. *ACS Photonics*. 2015. **2**, No 3. P. 326–333. https://doi.org/10.1021/ph5004237.
7. De Almeida J., Vasconcelos H., Jorge P., & Coelho L. Plasmonic optical fiber sensor based on double step growth of gold nano-islands. *Sensors*. 2018. **18**, No 4. P. 1267. https://doi.org/10.3390/s18041267.
8. Lee K.-S., El-Sayed M.A. Gold and silver nanoparticles in sensing and imaging: Sensitivity of plasmon response to size, shape, and metal composition. *J. Phys. Chem. B*. 2006. **110**, No 39. P. 19220–19225. https://doi.org/10.1021/jp062536y.

9. Garoli D., Calandrini E., Giovannini G., Hubarevich, A., Caligiuri, V., & De Angelis F. Nanoporous gold metamaterials for high sensitivity plasmonic sensing. *Nanoscale Horizons*. 2019. https://doi.org/10.1039/c9nh00168a.
10. Khlebtsov B., Khanadeev V., & Khlebtsov N. Tunable depolarized light scattering from gold and gold/silver nanorods. *Phys. Chem. Chem. Phys.* 2010. **12**, No 13. P. 3210. https://doi.org/10.1039/b925102b.
11. Garcia-Caurel E., De Martino A., Gaston J.-P., and Yan Li. Application of spectroscopic ellipsometry and Mueller ellipsometry to optical characterization. *Appl. Spectrosc*. 2013. **67**. P. 1–21.
12. Olmon R.L., Slovick B., Johnson T.W., Shelton D., Oh S.-H., Boreman G.D., & Raschke M.B. Optical dielectric function of gold. *Phys. Rev. B*. 2012. **86**, No 23. https://doi.org/10.1103/physrevb.86.235147.
13. Yampolskiy A.L., Makarenko O.V., Poperenko L.V., and Lysiuk V.O. Ellipsometry of hybrid noble metal-dielectric nanostructures. *Semiconductor Physics, Quantum Electronics and Optoelectronics*. 2018. **21**, No 4. P. 412. https://doi.org/10.15407/spqeo21.04.412.
14. Savenkov S.N. *Mueller-matrix Characterization of Biological Tissues*, vol. 2. Springer, NY, 2013.
15. Ambirajan A., Look D.C., Jr. Optimum angles for a Mueller matrix polarimeter. *Proc. SPIE*. 1994. **2265**, Polarization Analysis and Measurement II.
16. Holoborodko A.O., Krylov A.V., Robur L.I. Diagnostics of gold surface reconstruction by methods of multi-angle ellipsometry. *J. Nano- and Electron. Phys.* 2015. **7**, No 1. P. 01025 (6 pp.).

Authors and CV

Makarenko Olexiy Volodymyrovych, born in 1974, Candidate of Sciences in Physics and Mathematics in 2001. Working since 1997 as an engineer, Assistant Professor (2001) and then as Associate Professor (2005) at the Taras Shevchenko Kyiv National University. O.V. Makarenko is specialized in color, lens design and creating of optoelectronic devices, optics of inhomogeneous media and polarized light. He has more than 20 scientific publications.

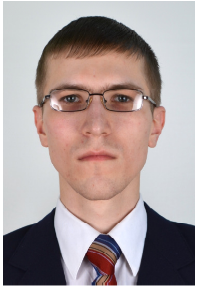

Yampolskiy Andriy Leonidovych, born in 1993, MSc in Physics (Laser and Optoelectronic Technique) in 2017. At present, PhD student in Physics and Astronomy of the Chair of Optics, Department of Physics, Taras Shevchenko Kyiv National University, Scientific interests: ellipsometry, optically anisotropic materials, nanotechnology, optoelectronics, experimental devices development.

Lendiel Vasyl Vasylyovych, born in 1956, in 1978 he graduated from the Faculty of Physics, Taras Shevchenko Kyiv National University, specializing in Optical Instruments and Spectroscopy, a leading engineer. Scientific interests: technology of thin films of various materials, their optical and electrophysical characteristics, nanotechnology.

Poperenko Leonid Volodymyrovych, Doctor of Sciences in Physics and Mathematics, Professor, Head of the Chair of Optics at the Department of Physics, Taras Shevchenko Kyiv National University. He has more than 200 publications. His research interests are ellipsometry, thin films, metal optics, ion implantation, plasmonics.

Lysiuk Viktor Oleksandrovych, born in 1980, received his PhD in Physics and Mathematics from the Taras Shevchenko Kyiv National University (2011) and senior scientific researcher title (2014). Senior Researcher at the Lab of Optics and Optoelectronic Registering Media, V. Lashkariov Institute of Semiconductor Physics, NAS of Ukraine. OSA Member. His research interests are ion implantation, thin films, plasmonics, ferroelectrics, and optical biosensors.